

Review of GaN Nanostructured Based Devices

Ahmed M. Nahhas*

Department of Electrical Engineering, Faculty of Engineering and Islamic Architecture, Umm Al Qura University, Makkah, Saudi Arabia
*Corresponding author: amnahas@uqu.edu.sa

Abstract This paper presents a review of recent advances of GaN based nanostructured materials and devices. GaN has gained substantial interest in the research area of wide band gap semiconductors due to its unique electrical, optical and structural properties. GaN nanostructured material exhibits many advantages for nanodevices due to its higher surface-to-volume ratio as compared to thin films. GaN nanostructured material has the ability to absorb ultraviolet (UV) radiation and immense in many optical applications. Recently, GaN nanostructured based devices have gained much attention due to their various potential applications. GaN as nanomaterial have been used in many devices such as UV photodetectors, light emitting diodes, solar cells and transistors. The recent aspects of GaN based devices are presented and discussed. The performance of several devices structures which has been demonstrated on GaN is reviewed. The structural, electrical, and optical properties are also reviewed.

Keywords: gallium nitride (GaN), nanostructured, doping, light emitting diodes, nanowires, multiple quantum wells, ultraviolet

Cite This Article: Ahmed M. Nahhas, "Review of GaN Nanostructured Based Devices." *American Journal of Nanomaterials*, vol. 6, no. 1 (2018): 1-14. doi: 10.12691/ajn-6-1-1.

1. Introduction

The group III-Nitride semiconductor materials have attracted a lot of interest for new generation of optoelectronic devices [1]. The advantage with these materials is the flexible bandgap varying from 0.7 to 6 eV hence covering an ultra-broad spectrum, from deep ultraviolet up to near infrared [2], allowing the development of numerous applications. Solar cells based on nitride materials have readily been investigated for terrestrial and space-based applications [3]. Transistors performance for high power electronics, ground-based communications and biological agent detection devices has been enhanced [4]. Major efforts have been dedicated to the technological fabrication in order to achieve efficient emitters and detectors [5]. Recent progress has demonstrated cutting edge results in high-speed data rate connectivity and integrated circuits [6]. Imaging sensors on high speed electronics have been implemented founded on their sensitive applications in security screening [7].

GaN as a member of group III-nitride family has become the revolutionary material owing to its electronic and optical properties. The direct, flexible and wide bandgap makes GaN materiel a key candidate for achieving high frequency, large bandwidth, high power and efficiency devices. GaN based detectors are in particular suitable for full color display, high density information storage, and UV communication links [8].

GaN is a very hard, chemically and mechanically stable wide bandgap (3.4 eV) semiconductor material with high heat capacity and thermal conductivity which makes it suitable to be used for sensors [9], for high power electronic devices such as field effect transistor (FET) [10]

and for optoelectronic devices such as light emitting diode (LED) [11]. The optical properties of GaN nanostructured are of great current interest because of the potential application in solid state lighting [12]. In *n*-type GaN, an UV peak at approximately 3.42 eV usually dominates the photoluminescence spectrum [13]. The blue luminescence at 2.7 to 3 eV peak energy has been extensively studied; this peak dominates due to optically active defects and impurities [14]. On the other hand, such defects can be destructive in a device. A well-engineered inorganic nanoparticle approach offers many advantages [15]. Meanwhile, in nanostructures having a large specific area, the surface states effect became significant in influencing the carrier recombination mechanism [16].

2. GaN Nanostructured Materials Doping

GaN nanostructured material exhibits many advantages for nanodevices because of its higher surface-to-volume ratio as compared to thin films. The GaN nanostructured material has ability to absorb UV radiation and immense in many optical applications [17]. GaN nanostructured have various shapes including nanowires [18], nanoparticles [19], nanobelts [20], nanorings [21], nanotubes [22], nanodots [23], and nanorods [24]. GaN nanoparticles generated lot of interest among scientists as well as technologists during past few years. The electronic properties of quantum confinement of electrons of nanoparticles make them very useful in electronic industry including many GaN applications [25].

GaN doping is very important for different devices structures. Several techniques have been used in GaN doping. The ion implantation technique for controlling *n*-

type or *p*-type conduction has been a significant challenge for GaN based high-power devices to achieve levels approaching their theoretical limits of performance [26]. Previous studies on *n*-type conduction of GaN through silicon ion implantation achieved 86% [27], and approximately 100% [28] of activation rate after annealing at 1250 and 1400 °C, respectively. Such high temperature annealing results in serious surface degradation of GaN due to decomposition [29], thereby needs a protective layer. However, it is difficult to make a proper choice of a protective layer which remains unaltered and is removable after annealing above 1200°C. Therefore, achieving the high activation rate at lower temperature is a very important practice. On the other hand, the Mg ion implantation for *p*-type conductivity is more challenging due to the higher temperature annealing required for electrical activation, resulting in a major difficulty protecting the surface [30]. The formation energy of Mg on the Ga site (MgGa) near the valence band is about 1 eV higher than that of SiGa at the Fermi level near the conduction band [31], which may explain the difference of required annealing temperature for different conduction types. The efficient *p*-type doping of GaN is in general a challenging task [32]. Despite the achievements in realization of good quality *p*-type GaN, the activation efficiency of Mg atoms is still as low as few percent. The *p*-type doping of GaN is typically performed during growth, while the reports on other doping techniques common in semiconductor processing such as ion implantation [33], and diffusion [34] have been scarce. The thermal stability and redistribution of the implanted dopants in GaN revealed that implanted Mg have shown a change in the concentration profile after annealing temperatures. Indeed, post implantation annealing of GaN at high temperatures, typically 1100-1400°C, is necessary both for Mg redistribution and activation as well as lattice recovery. However, annealing above 800-900°C induces severe damages at the GaN surface due to nitrogen desorption. Because of this high sensitivity to post implantation thermal treatments, protecting the GaN surface using a cap layer is mandatory to prevent the nitrogen desorption [35,36].

Recently, GaN was also be doped with carbon [37]. The Intentional doping of carbon on GaN can be done using a hydrocarbon precursor technique [38]. The extrinsic carbon doping delivers better dynamic properties for the device voltage capabilities. In some devices like GaN on silicon (Si) devices offer an optimal solution for efficient dc-dc conversion. Handling high voltage operation at high switching frequency, also have long shown clear advantage over their Si counterparts [39]. Due to the need of high blocking voltage, carbon compensation doping is the most commonly used method for achieving highly resistive GaN buffers. However, the heterostructure field effect transistors grown using carbon doped GaN suffer from serious setbacks, such as high dynamic on-resistance and slowly recovering current collapse [40]. Carbon doping has been traditionally achieved through incorporation of carbon originating from the metal organic precursor during the growth process [41,42] in a so called auto doping technique. To achieve high carbon concentrations, growth temperature, pressure, and V/III ratio had to be substantially decreased. This entailed inferior crystal quality leading to a higher dislocation density yielding lower blocking voltages and electron

mobility in the channel [43]. Lately, extrinsic carbon doping of GaN buffers has been gathering momentum as a method to incorporate carbon whilst maintaining growth parameters optimized for crystal quality.

GaN can also be doped with europium (Eu). It is an attractive alternative to InGaN for the red light LED, as the InN rich alloy has disappointingly low luminescence efficiency [44,45]. The active lumophore in the first successful GaN:Eu injection device [46] is the primary defect, Eu₂, an isolated Eu ion located on a Ga site, EuGa [47,48]. Association of EuGa with other defects produces a variety of centers; competition for excitation among the various rare earth related defects gives rise to ‘site multiplicity’ in solid state rare earth luminescence spectra [49].

Like wide-gap II–VI semiconductors, GaN exhibits self-compensation, so neutralization of acceptor doping by native donors, which is energetically favorable for the crystal. There is a clear experimental evidence that GaN:Mg(Zn) films and crystals have high resistivity or are *n*-type owing to the compensation of acceptor impurities by native defects or unintentional H and O impurities [50,51]. The thermodynamic analysis of the defect chemistry in GaN:Mg crystals [52] suggests that, under equilibrium growth conditions, a MgGa acceptor controlled *p*-type can only be achieved at N₂ pressures above 10⁴ MPa, in agreement with experimental data [53]. Magnesium is the only dopant capable of ensuring stable, reproducible *p*-type conduction in GaN [54]. Magnesium incorporation is accompanied by the formation of considerable amounts of intrinsic and extrinsic defects. Clearly, the incorporation of such centers has a significant effect on the electrical and luminescent properties of GaN:Mg [55]. Low temperature photoluminescence spectra of Mg-doped GaN films show broad emission bands in the range 2.8-3.3 eV, due to donor recombination [56,57].

GaN can also be doped with Manganese (Mn). The growth of homogeneously Mn-doped Ga_{1-x}Mn_xN thin films have been carried out at different temperatures [58]. A high dopant concentration and high carrier concentration are inherent advantages of that doping. Mn has low solubility in gallium and its group V compounds. That phase separation occurs in the growth of GaMnAs when concentrations of over 5% Mn and temperatures of a few hundred Celsius were used during the growth process [59]. This proved an obstacle to obtaining the required magnetic semiconductor film properties for device fabrication. The Pulsed laser deposition (PLD) can be used to prepare thin films from multicomponent targets and allows Mn concentrations in the GaN films to be controlled easily by varying the quantity of Mn included in the initial target preparation [60]. The growth conditions can be far from equilibrium, which offers the possibility of reaching higher Mn concentrations without phase separation [60].

3. Comparison of GaN Based Nanostructured Devices

3.1. GaN Nanostructured LEDs Devices

GaN nanostructured based LEDs have been used extensively as a new energy efficient and environment friendly light source for their promising applications in

displays, backlight units, laser diodes, traffic lights, and solid state lightening. GaN LEDs have a greater efficiency, long lifespan, high reliability, and many environmental benefits [61,62,63]. Recently, GaN LEDs have a great potential in automotive, medical, and display application including indoor, outdoor lighting, and signals. Nowadays, GaN based near-ultraviolet LEDs (NUV-LEDs) have attracted special attention with regard to pumping sources of white LEDs, photo catalysis, spectrometric detector and biochemical sensors [64,65,66,67]. While the demands for efficient blue GaN LEDs are high, the performance of blue GaN LEDs are seriously weakened by the critical problem of efficiency droop which refers to the reduction in internal quantum efficiency at high current densities [68].

GaN based LED structures consist of thin *p*-(Al)GaN/active layer/*n*-GaN epitaxial films on sapphire substrates [69]. However, the electrically injected mid- and deep-UV lasers based on conventional AlGaIn quantum wells (QWs) remain challenging because of valence sub bands crossover, difficult in *p*-type doping and material epitaxy growth. The requirements regarding the *p*-(Al)GaN layer are very diverse, including the high hole injection efficiency from the *p*-layer to the active layer, good electron blocking from the active layer to the *p*-layer, small bulk electrical resistance, good ohmic contact for the metal, and negligible optical loss [66-72].

The InGaN/GaN based LEDs have recently attracted great attention as efficient light sources for various applications [73,74]. They have found widespread commercial applications such as full color display, automotive headlights, mobile platforms and white solid state lamps and high light output power applications [75,76]. However, even in the case one achieves a higher light output power; it is often not clear what has caused the improvement. To understand how each experimental parameter influences optoelectronic performances of GaN based LEDs, a method of systematic analysis that assesses the interrelations independently and quantitatively is an absolute necessity. Some possible reasons responsible for efficiency droop which include Auger recombination [77], electron leakage from active region [77], poor hole injection in the device [78], polarization effect [79], and an inhomogeneous carrier distribution in active region [80]. Among them inefficient electron blocking, lower hole injection and an inhomogeneous carrier distribution in active region are recognized as primary causes for efficiency droop.

The actual mechanism of efficiency droop in InGaN/GaN LEDs still remains debatable, good crystal quality of the *p*-layer, high activation ratio of Mg for hole carriers. Also, little Mg diffusion from *p*- GaN into the InGaN QW during the high temperature epitaxial growth are considered to be the key technical issues [81,82]. Typically, such technical hurdles have been solved heuristically rather than analytically by changing various experimental parameters including epitaxial layer structures, epitaxial growth conditions (e.g., temperature, pressure, and growth speed), and annealing conditions of the *p*-layer (e.g., temperature and ambient gas), with a final goal of achieving higher light output power [83,84].

The vertically integrated group-III nitride based nanostructured LEDs have been designed and fabricated by Mikulics et al. [85]. For operation in the telecommunication wavelength range in the (*p*- GaN/InGaN/*n*-GaN/sapphire)

material system. The band edge luminescence energy of the nanostructured LEDs could be engineered by tuning the composition and size of the InGaN mesoscopic structures. Narrow band edge photoluminescence and electroluminescence was observed [85]. The InGaN structures feature a very low power consumption between 2 nW and 30 nW. The technological suitability process for the long term operation of LEDs was demonstrated by reliability measurements. The optical and the electrical characterization showed strong potential for the future low energy consumption optoelectronics [85]. The principal schematic of the integration technology of a single *p*-GaN/InGaN/*n*- GaN nanopyramid is shown in Figure 1 [85]. The E-beam lithography and RIE hole pattern transfer in SiO₂ layer/mask is shown in Figure 1(a). The selective area growth of InGaN nanopyramids is shown in Figure 1(b). The selective *p*-type GaN overgrowth by MOVPE is shown Figure 1(c). The recessed ohmic bottom contacts were processed by various lithography, dry etching, and annealing steps is shown in Figure 1(d) [85]. The dependence of the PL emission wavelength for InGaN nanopyramids on the calculated and the measured In composition is shown in Figure 2 [85]. The emission wavelength can be tuned from the UV range (GaN-365 nm) through the visible up to the near infrared range by controlling the trimethyl indium to total group III molar flow ratio. When using an In composition of close to 90%, emission is achieved in the technologically important telecommunication wavelength range [85].

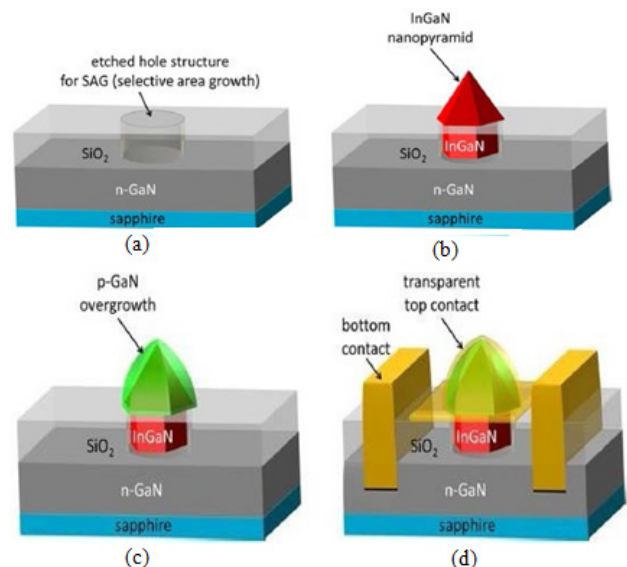


Figure 1. Principal schematics of the integration technology of a single *p*-GaN/InGaN/*n*-GaN nanopyramid: (a) E-beam lithography and RIE hole pattern transfer in SiO₂ layer/mask, (b) selective area growth of InGaN nanopyramids, (c) selective *p*-GaN overgrowth, (d) recessed ohmic bottom contacts [85]

The device concept for a hybrid nanocrystal/III-nitride based nanostructured LED was proposed by Gao et al. [86]. The approach was based on the direct electro-optical pumping of nanocrystals by electrically driven InGaN/GaN nanostructured LEDs as the primary excitation source. A universal hybrid optoelectronic platform was developed for a large range of optically active nano and mesoscopic structures. The advantage of the approach was that the emission of the nanocrystals can be electrically induced

without the need of contacting them [86]. The principal proof was demonstrated for the electro-optical pumping of CdSe nanocrystals. The nanostructured LEDs with a diameter of 100 nm exhibited a very low current of 8 nA at 5 V bias which is several orders of magnitude smaller than for those conventionally used. The leakage currents in the device layout were typically in the range of 8 to 20 pA/cm² at 5 V bias [86]. The principal schematics of the hybrid nanocrystal/III-nitride based nanostructured LED is shown in Figure 3 [86]. The fabrication schematics of the hybrid nanocrystal/III nitride based nano LED is shown in Figure 4 [86]. The micro PL intensity of nano LEDs with 100 (pink circles), 150 (blue circles), and 200 (red circles) nm diameter as a function of Ar-IBE accelerating voltage (Va) is shown in Figure 5. The highest intensity was observed for 200V accelerating voltage which was optimal for nano LED etching [86].

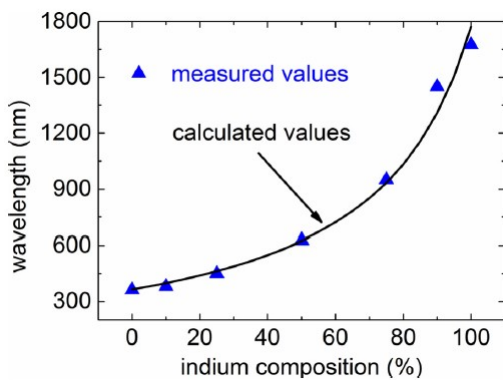


Figure 2. Dependence of the PL emission wavelength for InGaN nanopryamids on the In composition [85]

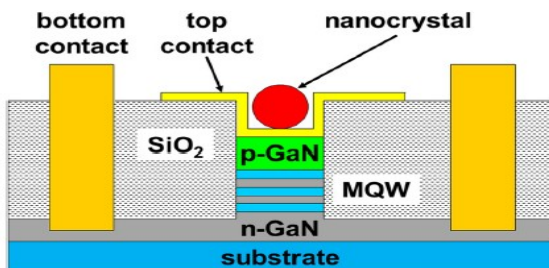


Figure 3. Principal schematics of the hybrid nanocrystal/III-nitride based nanostructured LED structure [86]

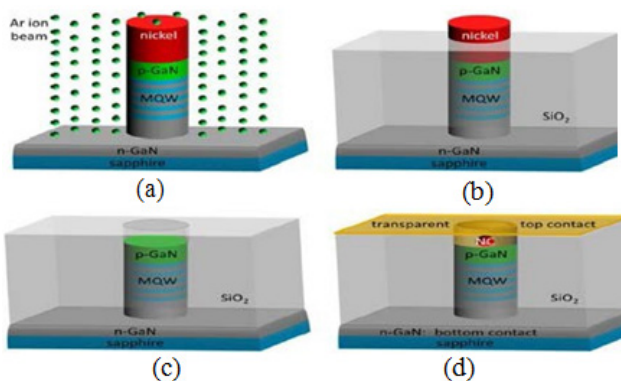


Figure 4. Fabrication schematics of the hybrid nanocrystal/III nitride based nano LED: (a) after Ar ion beam etching, (b) after encompassing the nanostructures in HSiQ/SiO₂ for device insulation, (c) after removal of the protective Ni masking cap (d) after formation of transparent top metal contact and nanocrystal integration [86]

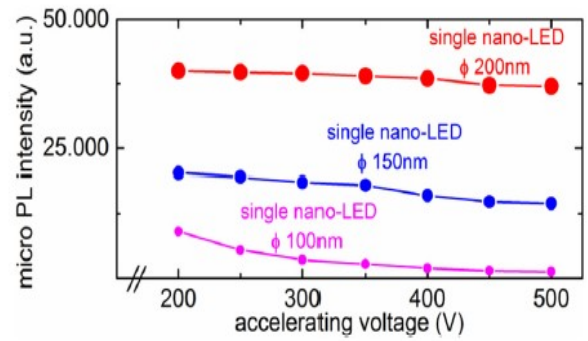


Figure 5. Micro PL intensity of nano LEDs with 100 (pink circles), 150 (blue circles), and 200 (red circles) nm diameter as a function of Ar-IBE Va [86]

The GaN based flip chip LED (FC LED) with an output power enhancement featuring conical structures was proposed by Liu et al. [87]. The GaN FCLED was fabricated by etching a self assembled monolayer SiO₂ spheres as the hard mask [87]. The roughening of the surface of FC LED components was found to increase the structural size of the components and elevates the light extraction efficiency of FC LED.

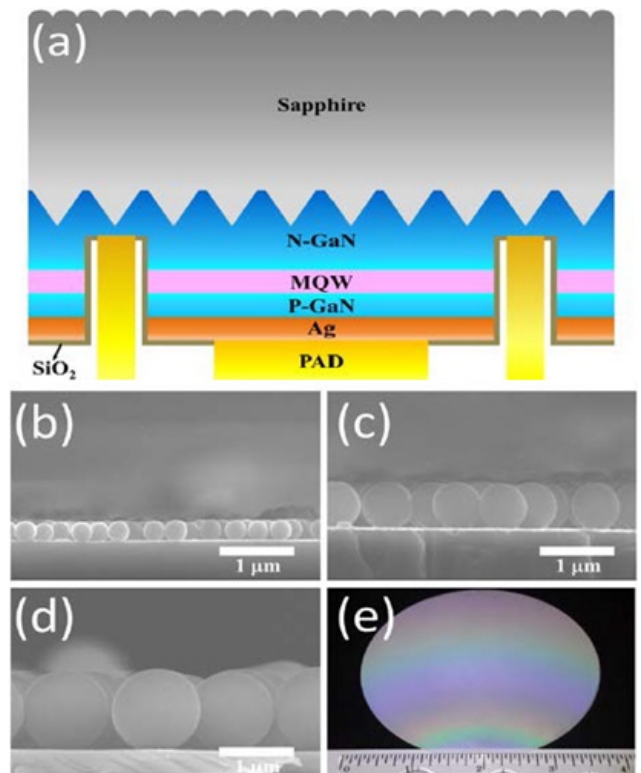


Figure 6. FC LED structure: (a) Schematic representation (b) 300 nm (c) 600 nm and (d) 1200 nm SiO₂ spheres single layer arrayed on the surface of sapphire (e) A full 4 in. FC LED wafer coated with 1200 nm SiO₂ sphere [87]

At a constant current of 400 mA, the output power of the FC LED with 1200 nm conical structures was 638.1 mW and enhanced by 6.1 % compared with the FC LED without surface roughening. In that study, SiO₂ spheres measuring 1200 nm in length were used to fabricate nano patterned sapphire flip chip (NPSFC) LED with a conical structure and a surface pattern of 1200 nm. The LED of the NPSFC was approximately 6.1 % higher than that of FC, verifying the feasibility of using nanosphere etching

techniques on improving FC LED efficiency [87]. The schematic representation of the FC LED structure is shown in Figure 6 (a).

Different scales of the SiO₂ spheres single layer arrayed on the surface of sapphire are shown in Figure 6 (b), (c), and (d) respectively [87]. The full 4 in FC LED wafer coated with 1200 nm SiO₂ sphere is shown in Figure 6 (e) [87]. The used SiO₂ spheres measuring at different scales as the etch stop layer and controlled etching times to produce NPSFC LED SEM results is shown in Figure 7 (a) 300 nm, and (b) 600 nm trapezoidal structure [87].

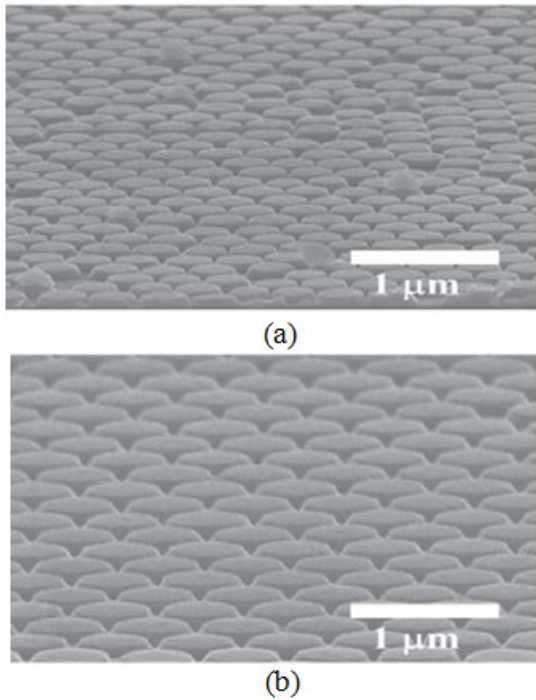


Figure 7. SEM of NPSFC LED: (a) 300 nm, and (b) 600 nm trapezoidal structure [87]

The designing and fabrication of *n*-ZnO/*p*-GaN heterojunction LEDs emitting diodes with a *p*-GaN/Al_{0.1}Ga_{0.9}N/*n*+GaN polarization induced tunneling junction (PITJ) were reported by Li et al. [88]. An intense and sharp ultraviolet emission centered at 396 nm was observed under forward bias. Compared with the *n*-ZnO/*p*-GaN reference diode without PITJ, the light intensity of the proposed diode was increased by 1.4 folds due to the improved current spreading. More importantly, the studied diode operates continuously for eight hours with the decay of only 3.5% under 20 mA, suggesting a remarkable operating stability [88]. The study's results demonstrated the feasibility of using PITJ as hole injection layer for high performance ZnO based light emitting devices [88]. The schematic diagram of the PITJ device is shown Figure 8 (a) [88]. The I-V characteristics of Au on *n*-ZnO, Ni/Au on *p*-GaN and In on *n*-GaN is shown in Figure 8 (b) [88]. The three linear curves shown in the figure reveal the good ohmic contacts of Au on ZnO, Au/Ni on *p*-GaN and In on *n*-GaN, which indicates the rectification behaviors arise from the heterojunctions [88]. The EL spectra of LED-1 under various forward bias voltages ranging from 10 V to 50V is shown in Figure 9 (a). Gaussian deconvolution of a representative EL spectrum from LED measured at 50 V is shown in Figure 9 (b). The EL spectra of LED-2 under

various forward bias voltages ranging from 10 V to 50 V is shown in Figure 9 (c). The relationship between the integrated EL intensity and voltage of two LEDs is shown in Figure 9 (d) [88].

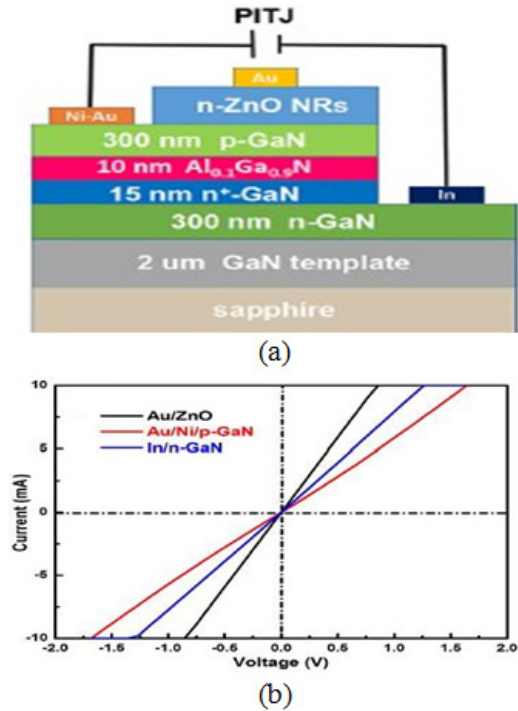


Figure 8. PITJ device: (a) Schematic diagram (b) I-V characteristics of Au on *n*-ZnO, Ni/Au on *p*-GaN and In on *n*-GaN [88]

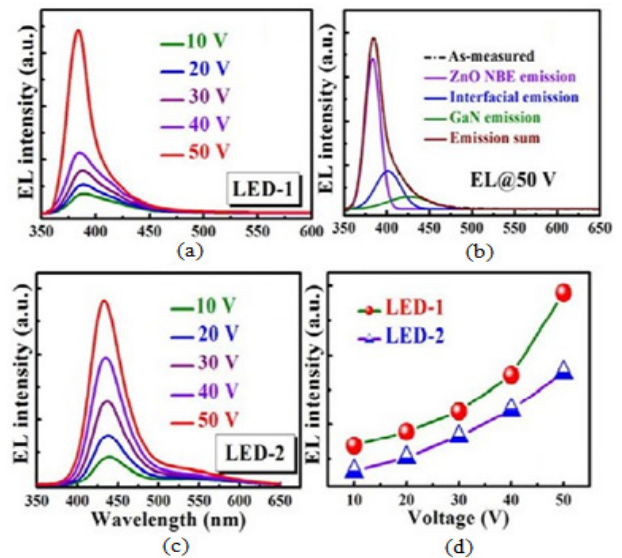


Figure 9. (a) EL spectra of LED under various forward bias voltages ranging from 10 V to 50 V (b) Gaussian deconvolution of a representative EL spectrum from LED measured at 50 V (c) EL spectra of LED under forward bias voltages ranging from 10 V to 50 V (d) Relationship between the integrated EL intensity and voltage of two LEDs [88]

The O-polar ZnO films grown on N-polar *p*-GaN/sapphire substrates and the heterojunction LEDs based O-polar *n*-ZnO/N-polar *p*-GaN were proposed and fabricated by Jiang et al. [89]. It was experimentally demonstrated that the interface polarization of O-polar *n*-ZnO/N-polar *p*-GaN heterojunction can shift the location of the depletion region from the interface deep into the ZnO side.

When a forward bias was applied to the proposed diode, a strong and high-purity UV emission located at 385 nm was observed. Compared with conventional Zn-polar n -ZnO/Ga-polar p -GaN heterostructure diode, the ultraviolet emission intensity of the proposed heterojunction diode was greatly enhanced due to the presence of polarization induced inversion layer at the ZnO side of the heterojunction interface. The highly efficient UV emission was confirmed in comparison with conventional Zn-polar n -ZnO/Ga-polar p -GaN heterojunction LEDs. The improved electroluminescence EL performance from the proposed diode was due the location of the depletion region shifts away from heterojunction interface deep into ZnO side due to the interface polarization [89]. The schematic drawing of O-polar n -ZnO/N-polar p -GaN heterostructure with a polarization-induced inversion layer (PIL) is shown in Figure 10 (a). Fixed charges induced by spontaneous (PSP) and piezoelectric (PPE) polarization is also displayed. shows the spatial distribution of fixed polarization charges and ionized dopants in O-polar n -ZnO/N-polar p -GaN heterostructure is shown in Figure 10 (b) [89]. The I-V characteristics curves of the LED are shown in Figure 11. The rectifying behavior with a turn-on voltage of about 3 V is observed. The linear curves from Au/Ni on p -GaN and Au on n -ZnO reveal good ohmic contacts at both electrodes, which indicates that the rectifying behavior of LED originated from the n -ZnO/ p -GaN heterojunction as shown in Figure 11 [89].

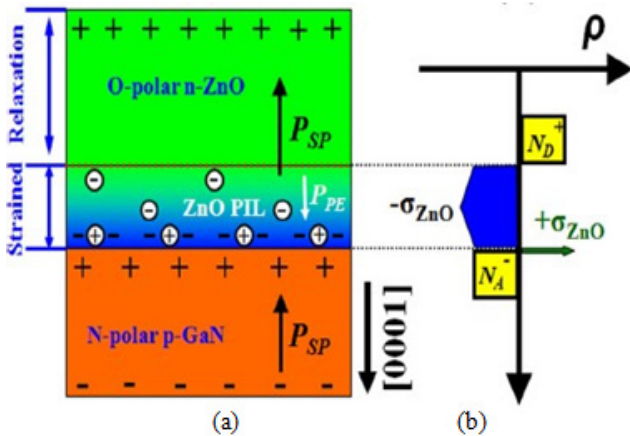


Figure 10. O-polar n -ZnO/N-polar p -GaN heterostructure with PIL: (a) Schematic drawing, Fixed charges induced by PSP and PPE polarization (b) Spatial distribution of fixed polarization charges and ionized dopants [89]

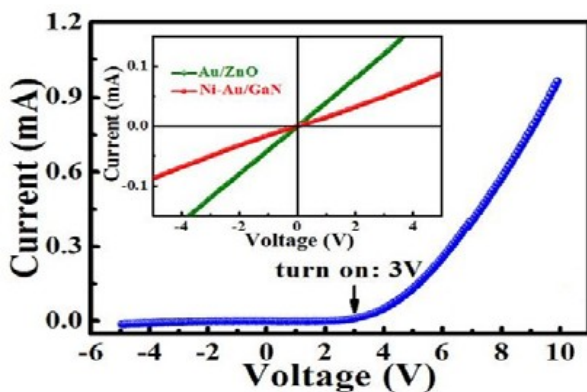


Figure 11. I-V characteristics of Au on n -ZnO, Ni/Au on p -GaN and In on n -GaN [89]

3.2. GaN Nanowires Devices

GaN nanowires have garnered much attention in recent years due to their attractive optical and electrical properties. GaN nanowires have been studied extensively [90]. GaN nanowires have been used as building units to construct different nano devices, such as nanolasers, detectors, and sensors [91]. Moreover, GaN nanowires lasers are attracting increasing research interest for ultra small coherent light sources [92]. GaN nanowires lasers are becoming key elements in a wide range of future applications, such as solid state lighting, spectroscopy, and on chip transmitters [93]. The lasing properties of GaN nanomaterials are very important for making useful practical applications.

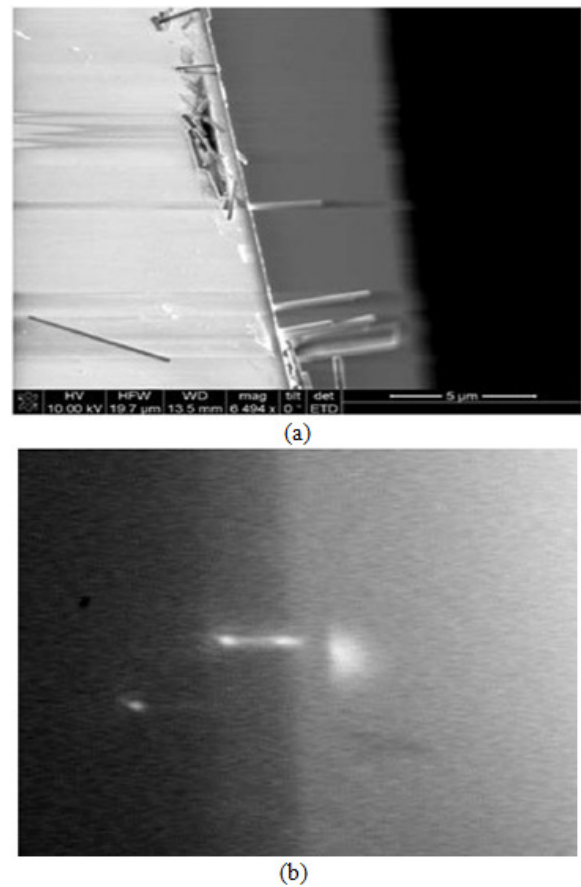


Figure 12. (a) SEM imaging of the GaN nanowires placed at the substrate's edge (b) CCD images of individual nanowires in lasing mode [94]

The polarization properties of GaN nanowires laser have been reported by Hurtado et al. [94]. The linear and the elliptical light polarizations were measured at different pumping strengths [94]. It has been observed that the switching between these two polarization states was also observed as the optical excitation was increased. This polarization switching was attributed to the change in the transverse modes due to their different cavity losses. It was found that the laser emission was occurring in two different wavelengths and with distinct light polarizations, linear and elliptical [94]. Furthermore, it was observed that the switching in the emitted light polarization from linear to elliptical polarization. These results offered promise for the design of novel polarized nanoscale lasers for use in polarization sensitive applications, such as all

optical signal processing at the nanoscale and atom trapping [94]. The SEM imaging of the GaN nanowires placed at the substrate's edge is shown in Figure 12 (a). The charge coupled device (CCD) images of individual nanowires in lasing mode is shown in Figure 12 (b) [94].

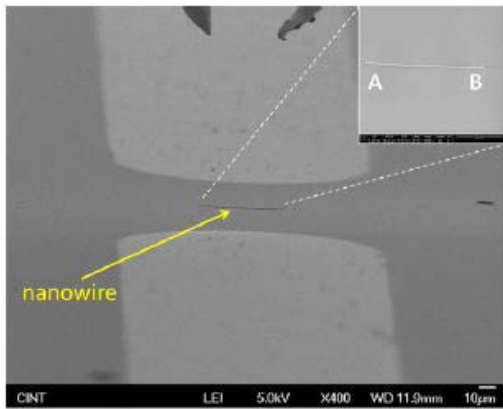


Figure 13. SEM image of a single GaN nanowires placed between gold patterns on a sapphire substrate using a nanomanipulator. The inset shows a magnified image of the nanowires, where “A” denotes the larger diameter end of the nanowires and “B” denotes the smaller diameter end [95]

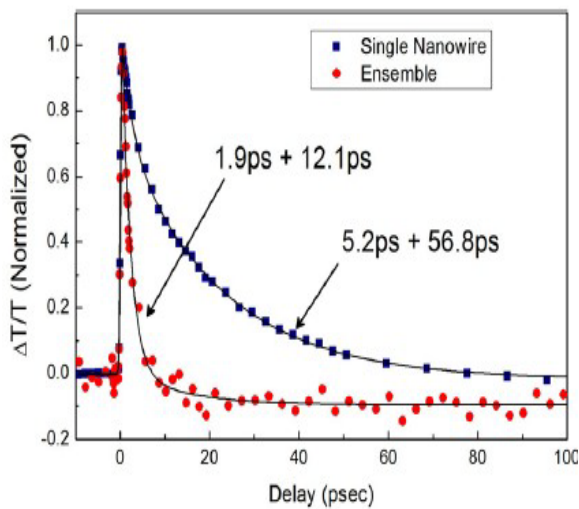


Figure 14. Normalized photoinduced transmission changes in the single and ensemble nanowires [95]

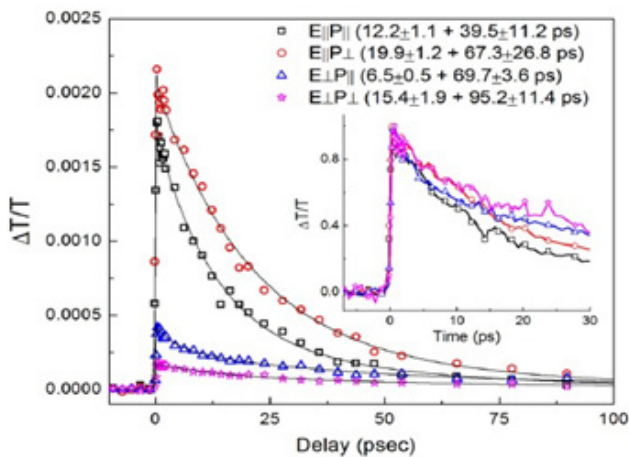


Figure 15. Polarization dependent transmission in the single GaN nanowires at a pump fluence of 510 $\mu\text{J}/\text{cm}^2$ and position P₂ on the nanowires, E and P denote the pump and probe polarizations [95]

The study of the ultrafast optical microscopy experiments on single GaN nanowires as a function of position, polarization, and pump fluence has been reported by Upadhyya et al. [95]. The study's aim was to understand the carrier transport, relaxation, and recombination in these quasi-one-dimensional GaN based nano systems [95]. This is therefore important in optimizing them for various applications. The study's result showed that the revealing density- dependent carrier relaxation that could be due to laser- induced transformation of gallium vacancy-related complexes. Also, the polarization dependent anisotropy in the relaxation dynamics was observed, due to the differences in absorption for light polarized parallel and perpendicular to the nanowire axis. Finally, the measurements revealed a surprising change in the positive differential transmission signal as the diameter varied along the nanowire corresponding to state filling on the larger end and induced absorption on the smaller end [95]. The SEM image of a single GaN nanowires placed between gold patterns on a sapphire substrate using a nanomanipulator is shown in Figure 13 [95]. The normalized photoinduced transmission changes in the single and ensemble nanowires with a pump fluence of 510 $\mu\text{J}/\text{cm}^2$ (corresponding to a carrier density of $1.82 \times 10^{20} \text{cm}^{-3}$) is shown in Figure 14. Both pump and probe were polarized parallel to the nanowires axis in the single nanowires measurements. The solid lines denote curve fits to the measured data, with the resulting time constants labeled for each trace [95]. The polarization dependent transmission in the single GaN nanowires is shown in Figure 15 [95].

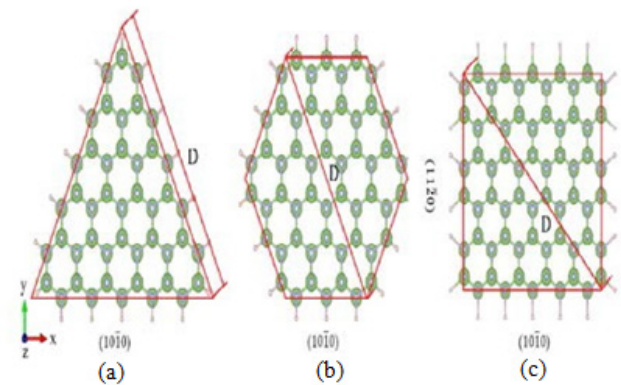


Figure 16. Atomistic structures of the GaN nanowires (a) Tri-GaN, (b) Hex-GaN (c) Rect-GaN [96]

The bandgap engineering has been a powerful technique for manipulating the electronic and optical properties of semiconductors. The electronic properties of GaN nanowires have been studied by Ming et al. [96]. In that study, a systematic investigation of the electronic properties of GaN nanowires was carried out using the density functional based tight binding method (DFTB). The effect of geometric structure and uniaxial strain on the electronic properties of GaN nanowires with diameters ranging from 0.8 to 10 nm have also been studied [96]. The study's results showed that the band gap of GaN nanowires depends linearly on both the surface to volume ratio (S/V) and tensile strain. The band gap of GaN nanowires increased linearly with S/V, while it decreased linearly with increasing tensile strain. These linear relationships provide an effect way in designing GaN

nanowires for their applications in novel nano devices [96]. The atomistic structures of the GaN nanowires are shown in Figure 16 (a) for Tri-GaN nanowires, (b) Hex-GaN nanowires, and (c) Rect-GaN nanowires. The red dash lines enclose the regions for definition of transverse size, D and cross sectional area, A . Ga, N and H atoms are represented in gray, blue and pink, respectively [96]. The band structure for Tri-GaN nanowires with (a) $D = 0.88$ nm and (b) $D = 7.34$ nm is shown in Figure 17 [96]. Figure 18 (a) shows the bandgap versus transverse dimension D and (b) shows the bandgap versus S/V . The red solid line is the best fit one with slope 0.417 ± 0.004 eV·nm. Inset of (b) is the bandgap versus S/V relation for Hex-GaN nanowires [96].

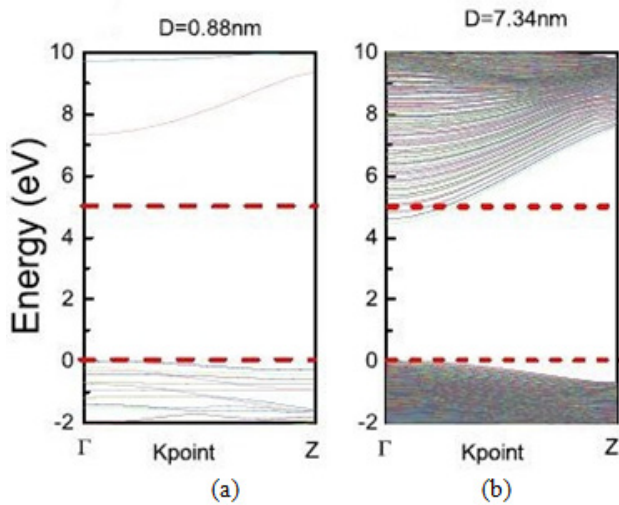


Figure 17. Band structure for Tri-GaN nanowires with (a) $D = 0.88$ nm and (b) $D = 7.34$ nm [96]

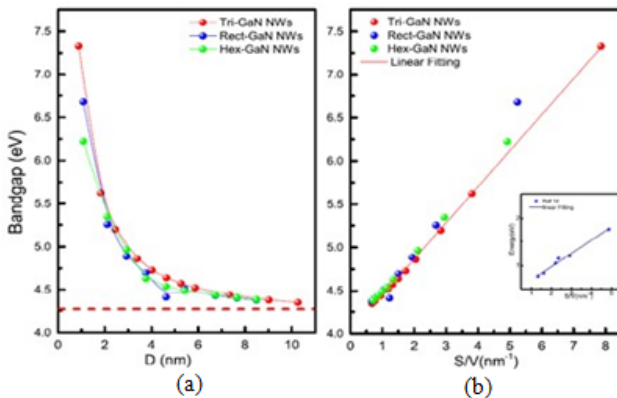


Figure 18. (a) Bandgap versus transverse dimension D (b) Bandgap versus S/V [96]

The fabrication and the characterization of GaN nanowires based vertical transistors have been demonstrated by Yu et al. [97]. The nanowires with smooth a-plane sidewalls have hexagonal geometry were made by top down etching. The nanowires transistor exhibited enhancement mode operation with threshold voltage of 1.2 V, on/off current ratio as high as 10^8 , and subthreshold slope as small as 68 mV/dec. Although there was a space charge limited current behavior at small source drain voltages, the drain current and transconductance reach up to 314 mA/mm and 125 mS/mm, respectively, when normalized with hexagonal nanowire circumference. The measured breakdown

voltage was around 140 V. This vertical approach provided a way to next generation GaN based power devices [97]. The study's results showed that the nanowires employing a top down approach have advantages in reliable c-axis orientation and smooth a-plane sidewalls. Because of their unique vertical design, these nanowires transistors exhibit promising performance in enhancement mode operation, large current output, high gain, and superior subthreshold behavior. Vertical nanoarchitectures are therefore suggested as a promising route for next generation GaN based power electronics [97]. The schematic of a vertical GaN transistor with three electrodes formed by mushroom shape nanowire array is shown in Figure 19 [97]. The SEM images of the GaN nanowires after wet chemical treatment is shown in Figure 20 [97].

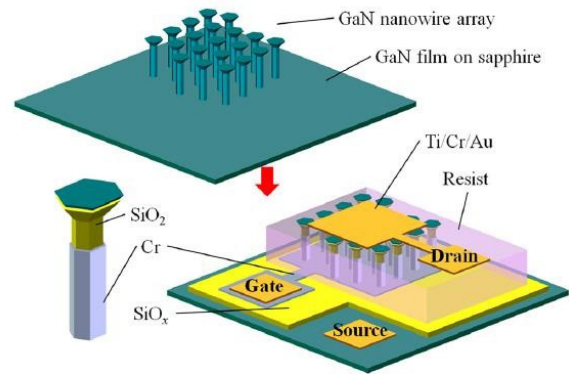


Figure 19. Schematic of a vertical GaN transistor with three electrodes [97]

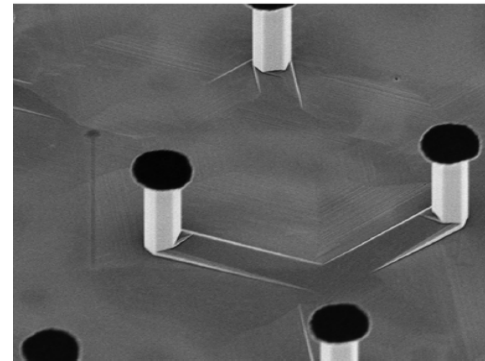


Figure 20. SEM images of GaN nanowires after wet chemical treatment [97]

The growth of GaN nanowires by molecular epitaxy on a Si substrate with nanoscale buffer layer of silicon carbide (SiC) has been reported by Reznik et al. [98]. The aim was to demonstrate the possibility of growing GaN nanowires on silicon substrates using SiC buffered layer and to compare the optical properties with the GaN nanowires grown on silicon directly without a buffered layer. The morphological and optical properties of the grown arrays were studied. It was found that the integral intensity of the photoluminescence of such structures is more than 2 times higher than the best nanowires GaN structures without buffer layer of silicon carbide. However, to extend the lifetime of GaN based optoelectronic devices and increase their perfection is highly desirable. The study's results showed that the intensity of the photoluminescence spectrum of the GaN nanowires on

SiC/Si(111) substrate integrally more than 2 times higher than that of the best structures of GaN nanowires without a buffer layer of SiC [98]. The extremely small width of GaN lines on Raman spectrum indicated high crystallographic quality GaN nanowires grown on SiC/Si open a new route using these structures in future optoelectronic applications [98]. The SEM images of the GaN nanowires on SiC/Si is shown in Figure 21 (a). The study's results can be further improved by using ZnO as a buffered layer due to the similar properties between GaN and ZnO. The PL spectra of GaN structures grown on Si of the GaN nanowires on SiC/Si is shown in Figure 21 (b) [98].

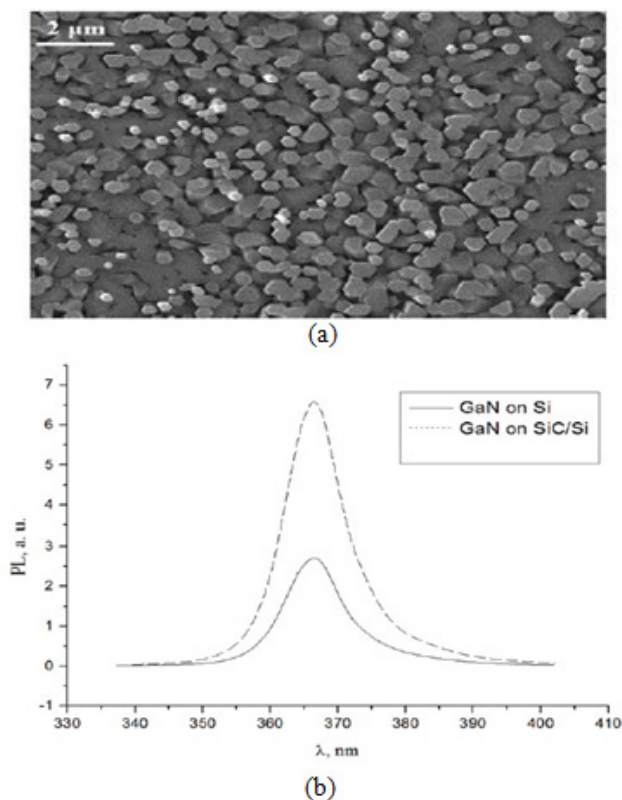


Figure 21. GaN nanowires on SiC/Si: (a) SEM images, (b) PL spectra of GaN structures grown on [98]

The epitaxy process of self organized GaN/AlGaIn nanowire heterostructures to achieve tunable emission in the deep UV spectral range was reported by Zhao et al. [99]. The self-organized AlGaIn nanowires have attracted significant attention for deep UV optoelectronics. However, due to the strong compositional modulations under conventional nitrogen rich growth conditions, emission wavelengths less than 250 nm have remained inaccessible. It was found that the Al-rich AlGaIn nanowires with much improved compositional uniformity can be achieved in a new growth paradigm, wherein a precise control on the optical bandgap of ternary AlGaIn nanowires can be achieved by varying the substrate temperature. The study's results showed that by employing a GaN nanowire template and growing AlGaIn nanowires with a low nitrogen flow rate, the Al/Ga compositional uniformity is significantly improved, and the optical bandgap (and thus the emission wavelength) of ternary AlGaIn nanowires can be readily tuned by varying the substrate temperature, instead by changing the Al/Ga BEP

ratio. These findings not only represent a critical step towards achieving UV LEDs and lasers below 240 nm with AlGaIn nanowire technologies but were also important for the growth and synthesis of other semiconductor nanostructures [99]. The growth schematic of AlGaIn nanowires segment on such GaN nanowire template is shown in Figure 22. The SEM image of GaN/AlGaIn nanowires on Si is shown in Figure 23 [99].

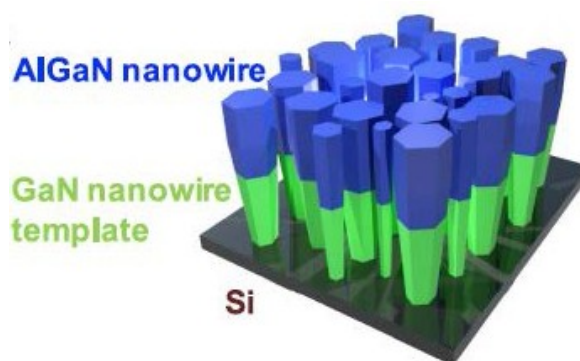


Figure 22. Growth schematic of AlGaIn nanowires segment on such GaN nanowire template [99]

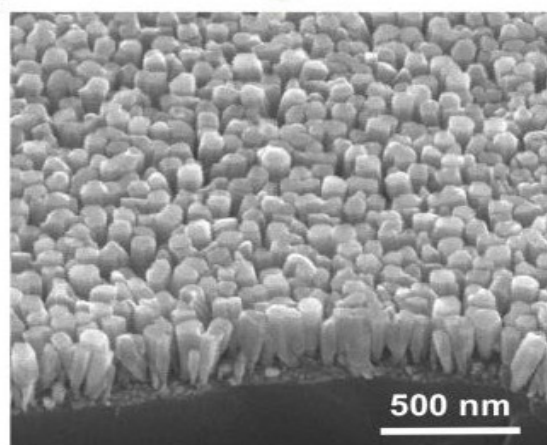


Figure 23. SEM image of GaN/AlGaIn nanowires on Si [99]

The lateral GaN nanowire gate all around transistor with top down process has been fabricated and characterized by Im et al. [100]. A triangle shaped GaN nanowire with 56 nm width was implemented on the GaN-on-insulator (GaNOI) wafer by utilizing buried oxide as sacrificial layer and anisotropic lateral wet etching of GaN in tetramethylammonium hydroxide solution [100]. During the subsequent GaN and AlGaIn epitaxy of source/drain planar regions, no growth occurred on the nanowire, due to self-limiting growth property. The study's results showed that the transistor exhibits normally-off operation with the threshold voltage of 3.5 V and promising performance: the maximum drain current of 0.11 mA, the maximum transconductance of 0.04 mS, the record off-state leakage current of 10^{-13} A/mm, and a very high on/off ratio of 108. It also showed that the top-down device concept using the GaNNOI wafer enables the fabrication of multiple parallel nanowires with positive threshold voltage and is advantageous compared with the bottom-up approach. The fabricated device with a nanowire height of 56 nm exhibited not only high on-state performances such

as $I_{d,max}$ of 0.11 mA and $g_{m,max}$ of 0.04 mS with high threshold voltage of 3.5 V but also excellent off-state features such as an extremely low leakage current of 10^{-13} A/mm and a very high I_{ON}/I_{off} ratio of 10^8 . These attractive on/off state characteristics are the full depletion result of the GAA (gate all around) nanowire, without the parasitic influence of GaN buffer layer. The GaN nanowire GAA transistor is very promising for nanoscale integrated CMOS circuits and high performance/high power application [100]. Figure 24 shows the schematic illustration of the of GaN nanowire GAA transistor fabrication sequence of a GaN nanowire GAA transistor. The schematic illustration of the of a GaN nanowire GAA transistor is shown Figure 24 (a). The structure of GaNOI wafer, prepared by smart cut technology is shown in Figure 24 (b) [100]. The formation of GaN nanowire arrays is shown in Figure 24 (c). The reduced GaN nanowire arrays achieved by etching along h1- 100i direction, which resulted in the triangle shaped nanowire is shown in Figure 24 (d). The release of GaN nanowire arrays by removing the sacrificial SiO_2 buried oxide is shown in Figure 24 (e). The regrowth of AlGaIn/GaN heterostructure on the patterned GaNOI wafer is shown in Figure 24 (f) [100].

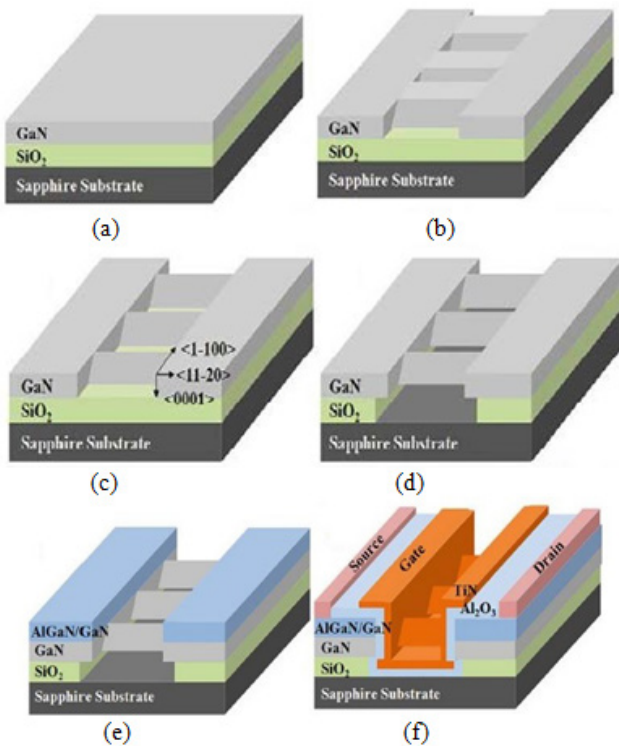


Figure 24. Schematic illustration of the of GaN nanowire GAA transistor fabrication sequence of a GaN nanowire GAA transistor: (a) Structure of GaNOI wafer (b) Formation of GaN nanowire arrays (c) Reduced GaN nanowire arrays (d) Release of GaN nanowire (e) Regrowth of AlGaIn/GaN heterostructure on the patterned GaNOI wafer (f) Schematic illustration of the nanodevice [100]

3.3. GaN Quantum Wells Devices

In the last decade, significant progress has been made in nitride based semiconductor devices, especially the blue LEDs with the InGaIn/GaN multiple quantum well (MQWs) structure as the active layer [101]. Based on that

progress, high-brightness GaN based LEDs are replacing the conventional lighting such as incandescent light bulbs and fluorescent lamps owing to their low power consumption and high energy conversion efficiency. However, issues still exist with regard to carrier recombination, transport, and distribution in the MQWs utilized in blue LED devices. Consequently, the devices suffer from reduction in external quantum efficiency (EQE) at high current densities. Achieving a higher efficiency at high current densities is necessary to expedite the use of LEDs as general lighting sources [102,103]. On the other hand, GaN based devices with InGaIn/GaN MQWs have attracted much interest due to their wide use in optoelectronics such as LED and laser diodes. However, the green InGaIn/GaN MQW LEDs are stepping into a bottleneck period because of high threading dislocations caused by lattice constants mismatch and thermal expansion coefficients between GaN based materials and substrates [104] and strong quantum stark effect (QCSE) [105]. All these can cause a heavy “efficiency droop” especially for green GaN based LEDs. To overcome and understand these problems further, many studies have been done in terms of the photoluminescence properties and carrier dynamics of InGaIn/GaN MQW LEDs series [106] grown on Si and sapphire. In contrast, the GaN based devices with AlGaIn QWs lasers has been limited to 320-360 nm [107], while only optically pumped deep UV lasers had been realized for shorter emission wavelength [108]. The challenges in realizing the electrically injected mid- and deep UV AlGaIn QWs lasers are attributed to the difficult growths of high Al content AlGaIn and *p*-AlN and the lack understanding on the physics of high Al content AlGaIn QWs.

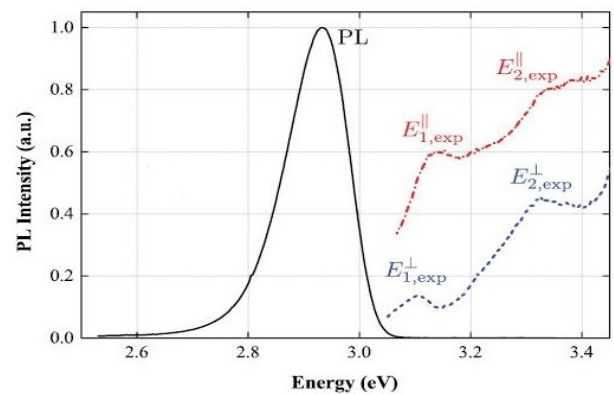


Figure 25. Low temperature (10 K) PL and PLE spectra for the m-plane InGaIn/GaN QW [109]

The study of the optical properties of m-plane InGaIn/GaN QWs was proposed Schulz et al. [109]. The InGaIn/GaN QWs were studied by PL and by photoluminescence excitation (PLE) spectroscopy at low temperature. The measured PL and PLE spectra have been compared with virtual crystal approximation (VCA) and atomistic tight binding (TB) calculations. The VCA does not produce a stoke shift (SS) since it neglects the effect of alloy disorder, but it reproduces the main features of PLE spectrum, e.g., the splitting of the exciton states. These features were also reproduced by the fully atomistic treatment. Moreover, a discernible SS was observed when including random alloy fluctuations [109]. The Low

temperature (10 K) PL and PLE spectra for the m-plane InGaN/GaN QW is shown Figure 25 [109].

The large spectral tunability of nitride on silicon MQWs for UV to visible microlasers, over a 200 nm spectral range was demonstrated by Selles et al. [110]. The comparison of different active layers and microdisk diameters were an evidence of the respective roles of the resonant or non resonant character of the optical excitation, of the defect density and the related room temperature emission efficiency, and of the QCSE. The broad tunability paved the way to the development of a UV visible integrated photonic platform embedding microlasers, possibly addressing multiple wavelengths [110]. The PL spectra of a 4 μm microdisk in the InGaN as a function of the pulsed laser excitation power is shown in Figure 26 [110].

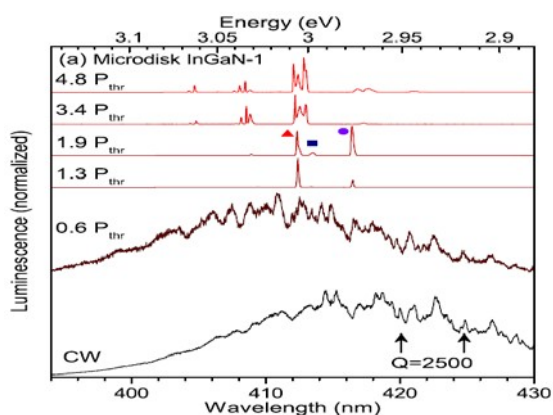


Figure 26. PL spectra of a 4 μm microdisk in the InGaN as a function of the pulsed laser excitation power [110]

The optical and structural properties of InGaN/GaN MQWs with different thicknesses of low temperature grown GaN cap layers was investigated by Yang et al. [111]. The study showed that the MQW emission energy red shifts and the peak intensity decreases with increasing GaN cap layer thickness, which may be partly caused by increased floating indium atoms accumulated at QW surface. They resulted in the increased interface roughness, higher defect density, and even lead to a thermal degradation of QW layers. An extra growth interruption introduced before the growth of GaN cap layer helped with evaporating the floating indium atoms, and therefore is an effective method to improve the optical properties of high indium content InGaN/GaN MQWs. The low temperature grown GaN cap (LT-cap) layer can effectively protect InGaN from decomposition. However, it was also found that with the increasing of cap layer thickness, the PL peak intensity was decreasing. This may be attributed to the floating indium atoms at the InGaN QW surface losing chance to evaporate when the cap layer gets thicker, which results in increased interface roughness, higher defect density, and even leads to a thermal degradation of QW layers. Thus, an extra interruption step directly after the QW growth to evaporate the floating indium was proposed, which can improve the performance remarkably while the emission energy of the QWs changes a little [111]. The cross sectional schematic of the InGaN/GaN MQWs epilayer structures is shown in Figure 27 (a). The LT cap layers is shown in Figure 27 (b) [111].

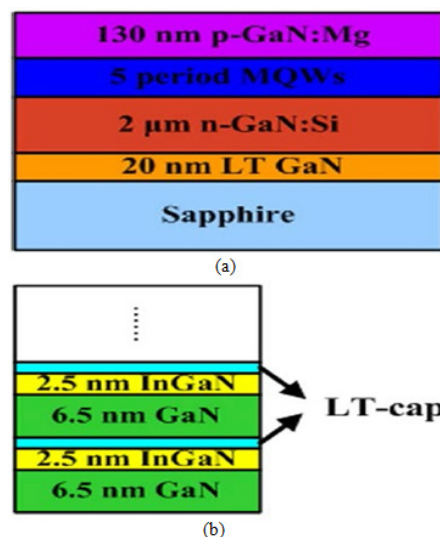


Figure 27. (a) Cross sectional schematic of the InGaN/GaN MQWs epilayer structures (b) LT cap layers [111]

4. Conclusion

GaN offers some potential in providing electronic and photonic devices, and also encouraging progress has been made in the research phase. Despite this progress, there are still number of important issues that are in need of further investigation before this material can be transitioned to commercial use for the stated applications. The task becomes more difficult by the highly successful GaN which competes for similar applications. GaN contributes to applications in optical devices, in part due to ease with which GaN can be produced in the nanostructures form. There is still much to be understood in terms of the mechanism of GaN based optical devices.

Although a number of GaN optical devices have been reported, there are some issues that need to be further investigation and study. These issues include the *p*-type doping, the lack of a credible *p*-type doping hampers widespread optical emitters in GaN. Furthermore, highly ionic nature of GaN with large electron photon coupling and low thermal conductivity does not bode well for GaN based electronic devices. Nanostructures seem a little easier to produce with GaN, but it remains to be checked whether nanostructures in general as hyped would really make inroads in the devices area. As for the nanostructures, GaN nanostructured including nanowires and nanorods provide a path to a new generation of devices, but a deliberate effort has to be expended for GaN nanostructured to be taken seriously for large scale device applications, and to achieve high device density with accessibility to individual nanodevices. Reliable methods for assembling and integrating building blocks into circuits need to be developed.

References

- [1] S. Madhusoodhanan, S. Sandoval, Y. Zhao, M. Ware, and Z. Chen, "A Highly linear temperature sensor using GaN-on-SiC heterojunction diode for high power applications," *IEEE Electron Device Letters* 38, 1105-1108 (2017).

- [2] Y. Guan, Y. Wang, D. Xu, and W. Wang, "A 1 MHz half-bridge resonant DC/DC converter based on GaN FETs and planar magnetics," *IEEE Transactions on Power Electronics* 32, 2876-2891 (2017).
- [3] J. Wu, W. Walukiewicz, K. Yu, W. Shan, and J. Ager, "Superior radiation resistance of In_{1-x}Ga_xN alloys: Full-solar-spectrum photovoltaic material system," *Journal of Applied Physics* 94, 6477-6482 (2003).
- [4] U. Mishra, L. Shen, T. Kazior, and Y. Wu, "GaN-based RF power devices and amplifiers," *Proceedings of IEEE* 96, 287-305 (2008).
- [5] R. Sun, G. Wang, and Z. Peng, "Fabrication and UV photoresponse of GaN nanowire-film hybrid films on sapphire substrates by chemical vapor deposition method," *Materials Letters* 217, 288-291 (2018).
- [6] V. Voronenkov, N. Bochkareva, R. Gorbunov, P. Latyshev, Y. Lelikov, Y. Rebane, A. Tsyuk, A. Zubrilov, and Y. Shreter, "Nature of V-shaped defects in GaN," *Japanese Journal of Applied Physics* 52, 08JE14 (2013).
- [7] C. Skierbiszewski, "Growth and characterization of AlInN/GaN quantum wells for high-speed intersubband devices at telecommunication wavelengths," *Proceedings of SPIE* 6121, 612109 (2006).
- [8] B. Gao, H. Liu, Q. Kuang, W. Zhou, and L. Cao, "A novel model of photo-carrier screening effect on the GaN-based p-i-n ultraviolet detector," *Science China Physics* 53, 793-801 (2010).
- [9] T. Zimmermann, M. Neuburger, P. Benkart, F. Hernandez-Guillen, C. Pietzka, M. Kunze, I. Daumiller, A. Dadgar, A. Krost, and E. Kohn, "Piezoelectric GaN sensor structures," *IEEE Electron Device Letters* 27, 309-312 (2006).
- [10] Y. Ikawa, K. Lee, J. Ao, and Y. Ohno, "Two-dimensional device simulation of AlGaIn/GaN heterojunction FET side-gating effect," *Japanese Journal of Applied Physics* 53, 114302 (2014).
- [11] H. Song and S. Lee, "Red light emitting solid state hybrid quantum dot-near-UV GaN LED devices," *Nanotechnology* 18, 255202 (2007).
- [12] S. Nakamura, "Current status of GaN-based solid-state lighting," *Materials Research* 34, 101-107 (2009).
- [13] K. Song and H. Kim, "Optical properties of undoped a-plane GaN grown with different initial growth pressures," *Japanese Journal of Applied Physics* 51, 092101 (2012).
- [14] M. Reshchikov and H. Morkoc, "Luminescence properties of defects in GaN," *Journal of Applied Physics* 97, 061301-061395 (2005).
- [15] A. Slimane, A. Najjar A, T. Ng, and B. Ooi, "Thermal annealing induced relaxation of compressive strain in porous GaN structures," *Proceedings of the 25th of IEEE Photonics Conference*, 921-922 (2012).
- [16] Z. Liao, H. Zhang, Y. Zhou, J. Xu, J. Zhang, and D. Yu, "Surface effects on photoluminescence of single ZnO nanowires," *Physics Letters A* 372, 4505-4509 (2008).
- [17] D. Li, X. Sun, and H. Song, "Realization of a high-performance GaN UV detector by nanoplasmonic enhancement," *Advanced Materials* 24, 845-849 (2012).
- [18] M. Hetzl, F. Schuster, A. Winerl, S. Weiszner, and M. Stutzmann, "GaN nanowires on diamond," *Materials Science in Semiconductor Processing* 48, 65-78 (2016).
- [19] M. Qaeed, K. Ibrahim, K. Saron, M. Mukhlif, A. Ismail, N. Elfadill, K. Chahrour, Q. Abdullah, and K. Andiroba, "New issue of GaN nanoparticles solar cell," *Current Applied Physics* 15, 499-503 (2015).
- [20] R. Yu, L. Dong, C. Pan, S. Niu, H. Liu, W. Liu, S. Chua, D. Chi, and Z. Wang, "Piezotronic effect on the transport properties of GaN nanobelts for active flexible electronics," *Advanced Materials* 24, 3532-3537 (2012).
- [21] Z. Li, X. Chen, H. Li, Q. Tu, Z. Yang, Y. Xu, and B. Hu, "Synthesis and Raman scattering of GaN nanorings, nanoribbons and nanowires," *Applied Physics A* 72, 629-632 (2001).
- [22] J. Sodre, E. Longo, C. Taft, J. Martins, and J. Santos, "Electronic structure of GaN nanotubes," *Comptes Rendus Chimie* 20, 190-196 (2017).
- [23] M. Lee, D. Mikulik, and S. Park, "Thick GaN growth via GaN nanodot formation by HVPE," *CrystEngComm* 19, 930-935 (2017).
- [24] M. Reddeppa, B. Park, S. Lee, N. Hai, M. Kim, and J. Oh, "Improved Schottky behavior of GaN nanorods using hydrogen plasma treatment," *Current Applied Physics* 17, 192-196 (2017).
- [25] S. Elashmawi, A. Abdelghany, and N. Hakeem, "Quantum confinement effect of CdS nanoparticles dispersed within PVP/PVA nanocomposites," *Journal of Materials Science* 24, 2956-2961 (2013).
- [26] T. Narita, K. Kataoka, M. Kanechika, T. Kachi, and T. Uesugi, "Ion implantation technique for conductivity control of GaN," *IEEE 17th International Workshop on Junction Technology (IWJT)*, 87-90 (2017).
- [27] S. Matsunaga, S. Yoshida, T. Kawaji, and T. Inada, "Silicon implantation in epitaxial GaN layers: Encapsulant annealing and electrical properties," *Journal of Applied Physics* 95, 2461 (2004).
- [28] Y. Irokawa, O. Fujishima, T. Kachi, and Y. Nakano, "Electrical activation characteristics of silicon implanted GaN," *Journal of Applied Physics* 97, 083505 (2005).
- [29] C. Ostermaier, P. Lager, M. Alomari, P. Herfurth, D. Maier, A. Alexewicz, M. Forte-Poisson, S. Delage, G. Strasser, D. Pogany, and E. Kohn, "Reliability investigation of the degradation of the surface passivation of InAlN/GaN HEMTs using a dual gate structure," *Microelectronics and Reliability* 52, 1812-1815 (2012).
- [30] Y. Kong, L. Liu, S. Xia, Y. Diao, H. Wang, and M. Wang, "Optoelectronic properties of Mg doping GaN nanowires," *Optical and Quantum Electronics* 48, 1-12 (2016).
- [31] C. Walle, J. Neugebauer, C. Stamp, M. McCluskey, and N. Johnson, "Defects and defect reactions in semiconductor nitrides," *Acta Physica Polonica A* 96, 613-627 (1999).
- [32] F. Naranjo, E. Calleja, Z. Bougrioua, A. Trampert, X. Kong, and K. Ploog, "Efficiency optimization of p-type doping in GaN:Mg layers grown by molecular-beam epitaxy," *Journal of Crystal Growth* 270, 542-546 (2004).
- [33] T. Narita, T. Kachi, K. Kataoka and T. Uesugi, "P-type doping of GaN(0001) by magnesium ion implantation," *Applied Physics Express* 10, 16501 (2017).
- [34] X. Cai, A. Djurisic, M. Xie, H. Liu, X. Zhang, J. Zhu, and H. Yang, "Ferromagnetism in Mn and Cr doped GaN by thermal diffusion," *Materials Science and Engineering B* 117, 292-295 (2005).
- [35] G. Aluri, M. Gowda, N. Mahadik, S. Sundaresan, M. Rao, J. Schreifels, J. Freitas, S. Qadri, and Y. Tian, "Microwave annealing of Mg-implanted and in situ Be-doped GaN," *Journal of Applied Physics* 108, 083103 (2010).
- [36] W. Khalfaoui, T. Oheix, G. El-Zammar, R. Benoit, F. Cayrel, E. Faulques, F. Massuyeau, A. Yvon, E. Collard, and D. Alquier, "Impact of rapid thermal annealing on Mg-implanted GaN with a SiO₂/AlN cap-layer," *Physica Status Solidi* 214, 1-8 (2017).
- [37] D. As, U. Kohler, M. Lubbers, J. Mimkes, and K. Lischka, "p-Type doping of cubic GaN by carbon," *Physica Status Solidi A* 188, 699-703 (2001).
- [38] H. Yacoub, C. Mauder, S. Leone, M. Eickelkamp, D. Fahle, M. Heuken, H. Kalisch, and A. Vescan, "Effect of different carbon doping techniques on the dynamic properties of GaN-on-Si buffers," *IEEE Transactions on Electron Devices* 64, 991-997 (2017).
- [39] D. Bisi, M. Meneghini, F. Marino, D. Marcon, S. Stoffels, M. Hove, S. Decoutere, G. Meneghesso, and E. Zanoni, "Kinetics of buffer-related R_{ON}-increase in GaN-on-Silicon MIS-HEMTs," *IEEE Electron Device Letters* 35, 1004-1006 (2014).
- [40] C. Seager, A. Wright, J. Yu, and W. Gotz, "Role of carbon in GaN," *Journal of Applied Physics* 92, 6553-6560 (2002).
- [41] H. Tang, J. Webb, J. Bardwell, S. Raymond, J. Salzman, and C. Uzan-Saguy, "Properties of carbon-doped GaN," *Applied Physics Letters* 78, 757-759 (2001).
- [42] D. Koleske, A. Wickenden, R. Henry, and M. Twigg, "Influence of MOVPE growth conditions on carbon and silicon concentrations in GaN," *Journal of Crystal Growth* 242, 55-69 (2002).
- [43] N. Weimann, L. Doppalapudi, H. Ng, and T. Moustakas, "Scattering of electrons at threading dislocations in GaN," *Journal of Applied Physics* 83, 3656-3659 (1998).
- [44] K. O'Donnell, P. Edwards, M. Kappers, K. Lorenz, E. Alves, and M. Bockowski, "Europium-doped GaN(Mg): beyond the limits of the light-emitting diode," *Physica Status Solidi C* 11, 662-665 (2014).
- [45] K. O'Donnell and B. Hourahine, "Rare earth doped III-nitrides for optoelectronics," *The European Physical Journal* 36, 91-103 (2006).

- [46] A. Nishikawa, T. Kawasaki, N. Furukawa, Y. Terai, and Y. Fujiwara, "Room-temperature red emission from a p-type/Europium-doped/n-type Gallium Nitride light-emitting diode under current injection," *Applied Physics Express* 2, 071004 (2009).
- [47] I. Roqan, K. O'Donnell, R. Martin, P. Edwards, S. Song, A. Vantomme, K. Lorenz, E. Alves, and M. Bockowski, "Identification of the prime optical center in GaN:Eu³⁺," *Physics Review B* 81, 085209 (2010).
- [48] K. Lorenz, E. Alves, I. Roqan, K. O'Donnell, A. Nishikawa, Y. Fujiwara, and M. Bockowski, "Lattice site location of optical centers in GaN:Eu light emitting diode material grown by organometallic vapor phase epitaxy," *Applied Physics Letters* 97, 111911 (2010).
- [49] V. Kachkanov, G. Laan, S. Dhessi, S. Cavill, M. Wallace, K. O'Donnell, and Y. Fujiwara, "Induced magnetic moment of Eu³⁺ ions in GaN," *Scientific Reports* 2, 969 (2012).
- [50] E. Litwin-Staszewska, T. Suski, R. Pietrkowski, I. Grzegory, and M. Bockowski, "Temperature dependence of electrical properties of Gallium-Nitride single crystals doped with Mg and their evolution with annealing," *Journal of Applied Physics* 89, 7960-7965 (2001).
- [51] I. Rogozin, A. Georgobiani, and M. Kotlyarevsky, " V_N -Mg defect complexes as compensating centers in GaN:Mg," *Inorganic Materials* 44, 1342-1347 (2008).
- [52] I. Rogozin, and A. Georgobiani "Theoretical analysis of defect formation in GaN:Mg crystals," *Bulletin of the Lebedev Physics Institute* 34, 3-13 (2007).
- [53] I. Akasaki, H. Amano, M. Kito, and K. Hiramatsu, "Photoluminescence of Mg-doped p-Type GaN and electroluminescence of GaN p-n Junction LED," *Journal of Luminescence* 48-49, 666-670 (1991).
- [54] S. Hashimoto, T. Nakamura, Y. Honda, and H. Amano, "Novel activation process for Mg-implanted GaN," *Journal of Crystal Growth* 388, 112-115 (2014).
- [55] L. Eckey, U. Gfuga, J. Holsta, A. Hoffmann, B. Schinellerb, K. Heimeb, M. Heukenc, O. Schonc, and R. Beccardc, "Compensation effects in Mg-doped GaN epilayers," *Journal of Crystal Growth* 189-190, 523-527 (1998).
- [56] M. Reshchikov, G. Yi, and B. Wesseles, "Behavior of 2.8- and 3.2-eV Photoluminescence bands in Mg-doped GaN at different temperatures and excitation densities," *Physics Review B* 59, 13176-13183 (1999).
- [57] S. Kim, J. Lee, C. Huh, N. Park, H. Kim, I. Lee, and S. Park, "Reactivation of Mg acceptor in Mg-doped GaN by nitrogen plasma treatment," *Applied Physics Letters* 76, 3079-308 (2000).
- [58] J. Sheu, P. Chen, C. Shin, M. Lee, P. Liao, and W. Lai, "Manganese-doped AlGaIn/GaN heterojunction solar cells with intermediate band absorption," *Solar Energy Materials and Solar Cells* 157, 727-732 (2016).
- [59] H. Ohno, "Making nonmagnetic semiconductors ferromagnetic," *Science* 281, 951-956 (1998).
- [60] D. Mahony, J. Lunney, G. Tobin, and E. McGlynn, "Pulsed laser deposition of manganese doped GaN thin films," *Solid State Electronics* 47, 533-537 (2003).
- [61] H. Jia, L. Guo, W. Wang, and H. Chen, "Recent progress in GaN-based light-emitting diodes," *Advanced Materials* 157, 4641-4646 (2009).
- [62] Y. Narukawa, M. Ichikawa, D. Sanga, M. Sano, and T. Mukai, "White light emitting diodes with super-high luminous efficacy," *Journal of Physics D: Applied Physics* 43, 354002 (2009).
- [63] H. Kim, S. Park, H. Hwang, and N. Park, "Lateral current transport path, a model for GaN-based light-emitting diodes: applications to practical device designs," *Applied Physics Letters* 81, 1326-1328 (2002).
- [64] Q. Wu, Z. Yang, Z. Zhao, M. Que, X. Wang, and Y. Wang, "Synthesis, crystal structure and luminescence properties of a $Y_2Si_2O_7N_2:Ce^{3+}$ phosphor for near-UV white LEDs," *Journal of Materials Chemistry C* 2, 4967-4973 (2014).
- [65] E. Repo, S. Rengaraj, S. Pulkka, E. Castangnoli, S. Suihkonen, M. Sopanen, and M. Sillanp, "Photocatalytic degradation of dyes by CdS microspheres under near UV and blue LED radiation," *Separation and Purification Technology* 120, 206-214 (2013).
- [66] S. Hong, C. Cho, S. Lee, S. Yim, W. Lim, S. Kim, and S. Park, "Localized surface plasmon-enhanced near-ultraviolet emission from InGaIn/GaN light-emitting diodes using silver and platinum nanoparticles," *Optics Express* 21, 3138-3144 (2013).
- [67] M. Fischer, M. Wahl, and G. Friedrichs, "Design and field application of a UV-LED based optical fiber biofilm sensor," *Biosensors and Bioelectronics* 33, 172-178 (2012).
- [68] W. Phillips, E. Thrush, Y. Zhang, and C. Humphreys, "Studies of efficiency droop in GaN based LEDs," *Physica Status Solidi C* 9, 765-769 (2012).
- [69] T. Okimoto, M. Tsukihara, K. Kataoka, A. Kato, K. Nishino, Y. Naoi, and S. Sakai, "GaN- and AlGaN-based UV-LEDs on sapphire by metal-organic chemical vapor deposition," *Physica Status Solidi C* 5, 3066-3068 (2008).
- [70] X. Li, D. Zhao, D. Jiang, Z. Liu, P. Chen, J. Zhu, L. Le, J. Yang, X. He, S. Zhang, B. Zhang, J. Liu, and H. Yang, "The significant effect of the thickness of Ni film on the performance of the Ni/Au Ohmic contact to p-GaN," *Journal of Applied Physics* 116, 163708 (2014).
- [71] S. Han, D. Lee, S. Lee, C. Cho, M. Kwon, S. Lee, D. Noh, D. Kim, Y. Kim, and S. Park, "Effect of electron blocking layer on efficiency droop in InGaIn/GaN multiple quantum well light-emitting diodes," *Applied Physics Letters* 94, 231123 (2009).
- [72] D. Xu, H. Yang, D. Zhao, S. Li, and R. Wu, "Room-temperature optical transitions in Mg-doped cubic GaN/GaAs(100) grown by metalorganic chemical vapor deposition," *Applied Physics Letters* 87, 2064-2066 (2000).
- [73] C. Jia, T. Yu, H. Lu, C. Zhong, Y. Sun, Y. Tong, and G. Zhang, "Performance improvement of GaN-based LEDs with step stage InGaIn/GaN strain relief layers in GaN-based blue LEDs," *Optics Express* 21, 8444-8449 (2013).
- [74] Z. Quan, L. Wang, C. Zheng, J. Liu, and F. Jiang, "Roles of V-shaped pits on the improvement of quantum efficiency in InGaIn/GaN multiple quantum well light-emitting diodes," *Journal of Applied Physics* 116, 183107 (2014).
- [75] J. Tsao, M. Crawford, M. Coltrin, A. Fischer, D. Koleske, G. Subramania, G. Wang, J. Wierer, and R. Karlicek, "Toward smart and ultra-efficient solid-state lighting," *Advanced Optical Materials* 2, 809-836 (2014).
- [76] J. Iveland, L. Martinelli, J. Peretti, J. Speck, and C. Weisbuch, "Direct measurement of Auger electrons emitted from a semiconductor light emitting diode under electrical injection: identification of the dominant mechanism for efficiency droop," *Physics Review Letters* 110, 177406-177415 (2013).
- [77] T. Lu, S. Li, C. Liu, K. Zhang, Y. Xu, J. Tong, L. Wu, H. Wang, X. Yang, Y. Yin, G. Xiao, and Y. Zhou, "Advantages of GaN based light emitting diodes with a p-InGaIn hole reservoir layer," *Applied Physics Letters* 100, 141106-141113 (2012).
- [78] Z. Ju, W. Liu, Z. Zhang, S. Tan, Y. Ji, Z. Kyaw, X. Zhang, S. Lu, Y. Zhang, B. Zhu, N. Hasanov, X. Sun, and H. Demir, "Improved hole distribution in InGaIn/GaN light emitting diodes with graded thickness quantum barriers," *Applied Physics Letters* 102, 243504-243513 (2013).
- [79] C. Qin, Y. Gu, X. Sun, X. Wang, and Y. Zhang, "Structural dependence of piezoelectric size effects and macroscopic polarization in ZnO nanowires: A first-principles study," *Nano Research* 8, 2073-2081 (2015).
- [80] C. Wang, S. Chang, P. Ku, J. Li, Y. Lan, C. Lin, H. Yang, H. Kuo, T. Lu, S. Wang, and C. Chang, "Hole transport improvement in InGaIn/GaN light emitting diodes by graded composition multiple quantum barriers," *Applied Physics Letters* 99, 171106-171113 (2011).
- [81] H. Kaufmann, P. Schlotter, H. Obloh, K. Kohler, and M. Maier, "Hole conductivity and compensation in epitaxial GaN:Mg layers," *Physics Review B* 62, 10867-10872 (2000).
- [82] Z. Ju, W. Liu, Z. Zhang, S. Tan, Y. Ji, Z. Kyaw, X. Zhang, S. Lu, Y. Zhang, B. Zhu, N. Hasanov, X. Sun, and H. Demir, "Improved hole distribution in InGaIn/GaN light emitting diodes with graded thickness quantum barriers," *Applied Physics Letters* 102, 243504-243513 (2013).
- [83] R. Vaxenburg, A. Rodina, E. Lifshitz, and A. Efros, "The role of polarization fields in Auger-induced efficiency droop in nitride based light-emitting diodes," *Applied Physics Letters* 103, 221111-221115 (2013).
- [84] H. Ryu and W. Choi, "Optimization of InGaIn/GaN superlattice structures for high-efficiency vertical blue light-emitting diodes," *Journal of Applied Physics* 114, 173101 (2013).
- [85] M. Mikulics, A. Winden, M. Marso, A. Moonshiram, H. Luth, D. Grutzmacher, and H. Hardtdegen, "Nano-light-emitting-diodes based on InGaIn mesoscopic structures for energy saving optoelectronics," *Applied Physics Letters* 109, 041103 (2016).

- [86] M. Mikulics, Y. Arango, A. Winden, R. Adam, A. Hardtdegen, D. Grutzmacher, E. Plinski, D. Gregusova, J. Novak, P. Kordos, A. Moonshiram, M. Marso, Z. Sofer, H. Luth, and H. Hardtdegen, "Direct electro-optical pumping for hybrid CdSe nanocrystal/III-nitride based nano-light emitting diodes," *Applied Physics Letters* 108, 061107 (2016).
- [87] M. Liu, C. Lin, and C. Chan, "Output power enhancement of GaN-based flip-chip light-emitting diodes via conical structures generated by a monolayer of nanospheres," *AIP Advances* 6, 115013 (2016).
- [88] L. Li, Y. Zhang, L. Yan, J. Jiang, X. Han, G. Deng, C. Chi, and J. Song, "n-ZnO/p-GaN heterojunction light emitting diodes featuring a buried polarization induced tunneling junction," *AIP Advances* 6, 125204 (2016).
- [89] J. Jiang, Y. Zhang, C. Chi, Z. Shi, L. Yan, P. Li, B. Zhang, and G. Du, "Improved ultraviolet emission performance from polarization-engineered n-ZnO/p-GaN heterojunction diode," *Applied Physics Letters* 108, 063505 (2016).
- [90] L. Geelhaar, C. Cheze, B. Jenichen, O. Brandt, C. Pfüller, S. Munch, R. Rothmund, S. Reitzenstein, A. Forchel, T. Kehagias, P. Komninou, G. Dimitrakopoulos, T. Karakostas, L. Lari, P. Chalker, M. Gass, and H. Riechert, "Properties of GaN Nanowires Grown by Molecular Beam Epitaxy," *IEEE Journal of Selected Topics in Quantum Electronics* 17, 878-888 (2011).
- [91] C. Li, S. Liu, T. Luk, J. Figiel, I. Brener, S. Brueckel and G. Wang, "Intrinsic polarization control in rectangular GaN nanowire lasers," *Nanoscale* 8, 5682-5687 (2016).
- [92] T. Kuykendall, A. Schwartzberg, and S. Aloni, "Gallium nitride nanowires and heterostructures: Toward Color-Tunable and White Light Sources," *Advanced Materials* 27, 5805-5812 (2015).
- [93] Y. Song, R. Zhu, and Y. Wang, "Active noise filtering for X-band GaN transmitters with bitstream Modulations," *IEEE Transactions on Microwave Theory and Techniques* 65, 1-9 (2017).
- [94] A. Hurtado, H. Xu, J. Wright, S. Liu, Q. Li, G. Wang, T. Luk, J. Figiel, K. Cross, G. Balakrishnan, L. Lester, and I. Brener, "Polarization switching in GaN nanowire lasers," *Applied Physics Letters* 103, 251107 (2013).
- [95] P. Upadhyaya, J. Martinez, Q. Li, G. Wang, B. Swartzentruber, A. Taylor, and R. Prasankumar, "Space and time resolved spectroscopy of single GaN nanowires," *Applied Physics Letters* 106, 263103 (2015).
- [96] B. Ming, R. Wang, C. Yam, L. Xu, W. Lau, and H. Yan, "Bandgap engineering of GaN nanowires," *AIP Advances* 6, 055018 (2016).
- [97] F. Yu, D. Rummel, J. Hartmann, L. Caccamo, T. Schimpke, M. Strassburg, A. Gad, A. Bakin, H. Wehmann, B. Witzigmann, H. Wasisto, and A. Waag, "Vertical architecture for enhanced mode power transistors based on GaN nanowires," *Applied Physics Letters* 108, 213503 (2016).
- [98] R. Reznik, K. Kotlyar, I. Ilkiv, I. Soshnikov, S. Kukushkin, A. Osipov, E. Nikitina, and G. Cirilin, "MBE growth and optical properties of GaN nanowires on SiC/Si(111) hybrid substrate," *AIP Conference Proceedings* 1748, 040003 (2016).
- [99] S. Zhao, S. Woo, S. Sadaf, Y. Wu, A. Pofelski, D. Laleyan, R. Rashid, Y. Wang, G. Botton, and Z. Mi, "Molecular beam epitaxy growth of Al-rich AlGaIn nanowires for deep ultraviolet optoelectronics," *Applied Materials* 4, 086115 (2016).
- [100] K. Im, C. Won, S. Vodapally, R. Caulmilone, S. Cristoloveanu, Y. Kim, and J. Lee, "Fabrication of normally-off GaN nanowire gate-all-around FET with top-down approach," *Applied Physics Letters* 109, 143106 (2016).
- [101] A. Laubsch, M. Sabathil, J. Baur, M. Peter, and B. Hahn, "High-power and high-efficiency InGaIn-based light emitters," *IEEE Transactions on Electron Devices* 57, 79-87 (2010).
- [102] L. Wang, Z. Zhang, and N. Wang, "Current crowding phenomenon: Theoretical and direct correlation with the efficiency drop of light emitting diodes by a modified ABC model," *IEEE Journal of Quantum Electronics* 51, 1-9 (2015).
- [103] J. Cho, E. Schubert, and J. Kim, "Efficiency droop in light emitting diodes: Challenges and countermeasures," *Laser Photonics Review* 7, 408-421 (2012).
- [104] L. Liu, L. Wang, N. Liu, W. Yang, D. Li, W. Chen, Z. Feng, Y. Lee, L. Ferguson, and X. Hu, "Investigation of the light emission properties and carrier dynamics in dual-wavelength InGaIn/GaN multiple-quantum well light emitting diodes," *Journal of Applied Physics* 112, 083101 (2012).
- [105] E. Yu, G. Sullivan, P. Asbeck, C. Wang, D. Qiao, and S. Lau, "Measurement of piezoelectrically induced charge in GaN/AlGaIn heterostructure field-effect transistors," *Applied Physics Letters* 71, 2794 (1997).
- [106] S. Valdeza-Felip, L. Rigutti, F. Naranjo, P. Ruterana, J. Mangeney, F. Julien, M. Gonzalez-Herraez, and E. Monroy, "Carrier localization in InN/InGaIn multiple-quantum wells with high In-content," *Applied Physics Letters* 101, 062109 (2012).
- [107] S. Liu, P. Li, W. Lan, and W. Lin, "Improvements of AlGaIn/GaN p-i-n UV sensors with graded AlGaIn layer for the UV-B (280-320 nm) detection," *Materials Science and Engineering B* 122, 196-200 (2005).
- [108] V. Jmerik, E. Lutsenko, and S. Ivanov, "Plasma-assisted molecular beam epitaxy of AlGaIn heterostructures for deep-ultraviolet optically pumped lasers," *Physica Status Solidi A* 210, 439-450 (2013).
- [109] S. Schulz, D. Tanner, E. O'Reilly, M. Caro, F. Tang, J. Griffiths, F. Oehler, M. Kappers, R. Oliver, C. Humphreys, D. Sutherland, M. Davies, and P. Dawson, "Theoretical and experimental analysis of the photoluminescence and photoluminescence excitation spectroscopy spectra of m-plane InGaIn/GaN quantum wells," *Applied Physics Letters* 109, 223102 (2016).
- [110] J. Selles, V. Crepel, I. Roland, M. El Kurdi, X. Checoury, P. Boucaud, M. Mexis, M. Leroux, B. Damilano, S. Rennesson, F. Semond, B. Gayral, C. Brimont, and T. Guillet, "III-Nitride-on-silicon microdisk lasers from the blue to the deep ultra-violet," *Applied Physics Letters* 109, 231101 (2016).
- [111] J. Yang, D. Zhao, D. Jiang, P. Chen, J. Zhu, Z. Liu, L. Le, X. Li, X. He, J. Liu, H. Yang, Y. Zhang, and G. Du, "Optical and structural characteristics of high indium content InGaIn/GaN multi-quantum wells with varying GaIn cap layer thickness," *Journal of Applied Physics* 117, 055709 (2015).